Continental Shelf Research 30 (2010) 1730–1742

Contents lists available at ScienceDirect

Continental Shelf Research

journal homepage: www.elsevier.com/locate/csr

Temporal variability of the physical and chemical water characteristics at a coastal monitoring observatory: Station ENSENADA

L. Linacre [a,*], R. Durazo [b], J.M. Hernández-Ayón [c], F. Delgadillo-Hinojosa [c], G. Cervantes-Díaz [b], J.R. Lara-Lara [d], V. Camacho-Ibar [c], A. Siqueiros-Valencia [c], C. Bazán-Guzmán [d]

[a] Programa de Doctorado en Oceanografía Costera, Facultad de Ciencias Marinas/Instituto de Investigaciones Oceanológicas, Universidad Autónoma de Baja California (UABC), Km 107 Carretera Tijuana-Ensenada, Ensenada CP 22860, Baja California, México
[b] Facultad de Ciencias Marinas, UABC, Km 107 Carretera Tijuana-Ensenada, Ensenada CP 22860, Baja California, México
[c] Instituto de Investigaciones Oceanológicas, UABC, Km 107 Carretera Tijuana-Ensenada, Ensenada CP 22860, Baja California, México
[d] División de Oceanología, Departamento de Oceanografía Biológica, Centro de Investigación Científica y de Educación Superior de Ensenada (CICESE), Km 107 Carretera Tijuana-Ensenada, Ensenada CP 22860, Baja California, México

ARTICLE INFO

Article history:
Received 30 October 2009
Received in revised form
19 May 2010
Accepted 20 July 2010
Available online 24 July 2010

Keywords:
Time series
Station ENSENADA
Temporal variability
California current system
El Niño/La Niña
Baja California

ABSTRACT

The temporal variability of the physical and chemical conditions of coastal waters off Ensenada, Baja California (Mexico) was characterized. A historical analysis was made based on 11 years (1998–2008) of temperature and salinity data records measured quarterly by IMECOCAL, along a transect perpendicular to the coast (CalCOFI line 100). Moreover, the physical and chemical conditions at a coastal monitoring observatory called station ENSENADA were described using a 2-year data series (October 2006–November 2008) obtained with improved temporal resolution. The historical analysis of line 100 showed marked seasonal variability in the thermohaline conditions associated with fluctuations in the flow of the equatorward California Current and the poleward California Undercurrent, as well as with coastal upwelling events whose magnitude and frequency increase towards spring–summer. Interannual variability was also observed, related to warm and/or cold ENSO phases that modify the characteristics of the water column in this coastal region. The most striking characteristics of the interannual variability at station ENSENADA were La Niña conditions recorded from summer 2007 to mid 2008. During this cold ENSO phase, temperature, salinity, dissolved oxygen, density, and dissolved inorganic carbon data revealed the anomalous presence of subsurface water at the surface layers in spring 2008. Results suggest that the coastal observatory is sensitive to the temporal variability of hydrographic conditions on shelf coastal waters (<50 km) off Ensenada in the northern BC region. Consequently, station ENSENADA would be a good location to high-frequency monitors the oceanographic conditions of the transitional region between tropical/subtropical and subarctic systems of the California Current System.

1. Introduction

The California Current System (CCS) is one of the eastern boundary current systems that sustains the most productive ecosystems of the world, mainly due to alongshore winds that generate the upwelling of cold, relatively salty, nutrient-rich waters into the euphotic zone of coastal areas. Much of the knowledge of the CCS off the western coast of the Baja California (BC) peninsula has been obtained through the analysis of hydrographic data collected between 1950 and 1978 by the California Cooperative Oceanic Fisheries Investigations (CalCOFI) program and, since 1997, by the Mexican California Current Investigations (Investigaciones Mexicanas de la Corriente de California, IMECOCAL) program. Additionally, other sporadic studies carried out off the northwestern region of BC have described the hydrographic variability of coastal waters (Barton, 1985; Barton and Argote, 1980; Pérez-Brunius et al., 2006).

In the coastal domain of the CCS off northern BC, two water masses are transported at the surface and subsurface levels. The California Current (CC), a year-round equatorward surface flow, transports Subarctic Water (SAW), characterized by a relative minimum of salinity, high dissolved oxygen content, and a density range from 24.5 to 25.5 kg m^{-3}.The California Undercurrent (CU),

* Corresponding author. Tel.: +52 646 174 4570, +52 646 175 0500x24306; fax: +52 646 174 4103.
E-mail addresses: lorenalinacre@gmail.com, llinacre@uabc.mx (L. Linacre), rdurazo@uabc.edu.mx (R. Durazo), jmartin@uabc.edu.mx (J.M. Hernández-Ayón), fdelgadillo@uabc.edu.mx (F. Delgadillo-Hinojosa), gabita23@gmail.com (G. Cervantes-Díaz), rlara@cicese.mx (J.R. Lara-Lara), vcamacho@uabc.edu.mx (V. Camacho-Ibar), arsiva@uabc.edu.mx (A. Siqueiros-Valencia), cbazan@cicese.mx (C. Bazán-Guzmán).

0278-4343/$ - see front matter © 2010 Elsevier Ltd. All rights reserved.
doi:10.1016/j.csr.2010.07.011

a poleward subsurface (100–400 m) flow that transports Equatorial Subsurface Water (ESsW), characterized by relatively high salinity, high nutrient concentration, and low dissolved oxygen content. Its core of relative maximum salinity is normally confined over the continental slope of the northern and central coast of BC, around the 26.5 kg m^{-3} isopycnal surface (Hickey, 1979; Barton and Argote, 1980; Lynn and Simpson, 1987; Durazo and Baumgartner, 2002; Durazo et al., 2010). A third surface poleward flow has been described within 200 km of the southern California coast as a northward branch of the CC. This is the Inshore Current or California Countercurrent (Lynn and Simpson, 1987). Although the presence of this near surface flow has not been documented off BC at seasonal scales (Lynn and Simpson, 1987; Durazo et al., 2010), surface poleward flows along the continental shelf have been associated with low temperature and small-scale (20–50 km) coastal cyclonic features (Durazo and Baumgartner, 2002; Durazo et al., 2005). Additionally, sustained surface poleward flows have been reported in the continental shelf off Tijuana at 32.5°N (Alvarez et al., 1990), near 30°50′N (Barton, 1985), and at 31.3°N (Alvarez et al., 1984).

Northwesterly winds prevail in the region during most of the year. As a consequence, coastal upwelling events occur year-round off BC. These winds are more intense in spring when the coastal upwelling events are stronger and more frequent (Bakun and Nelson, 1977; Huyer, 1983; Pérez-Brunius et al., 2007; Castro and Martínez, 2010). Additionally, positive wind stress curl near the continental margins in the BC region generates Ekman pumping that brings salty CU waters toward the surface at the coastal regions (Castro and Martínez, 2010).

Climatological analyses of the hydrographic time series have shown that the distribution of properties of CCS water is determined mainly by seasonal to decadal variability (Hickey, 1979; Lynn and Simpson, 1987; Bograd and Lynn, 2003). Seasonal fluctuations have been reported for surface and subsurface flows of the CCS. Off northern BC, the surface equatorward flow intensifies in a coastal jet during spring, while the subsurface poleward flow is practically non-existent in coastal waters or may be located deeper or displaced westward (Bograd and Lynn, 2003; Lynn et al., 2003; Durazo et al., 2010). Towards summer–autumn, the CC is characterized by enhanced mesoscale activity, with gyres and eddies developing along its southward displacement. Likewise, the poleward flow of the CU intensifies during summer–early autumn (Lynn and Simpson, 1987; Soto-Mardones et al., 2004; Jeronimo and Gómez-Valdés, 2007; Durazo et al., 2010). At the interannual time scale, variability observed in the thermohaline conditions of the CCS has been closely linked to remote large-scale forcings with effects in the warming or cooling of local waters during El Niño and La Niña, respectively, mainly due to anomalies in the regional flows and in the intensity of coastal upwelling, as well as changes in water transports modulated by long-term fluctuations in wind patterns (Pérez-Brunius et al., 2006; Durazo, 2009). Particularly at the upper ocean, mixed layer temperature and salinity have demonstrated interannual variability mainly associated with regional (northern and southern BC) differences in the atmosphere–ocean net heat fluxes and with large-scale variability in the sea surface height anomaly, respectively (Gómez-Valdés and Jeronimo, 2009).

Although extensive programs like CalCOFI and IMECOCAL and some other local efforts have generated a comprehensive description of the CCS off BC, they were obtained from data series with low temporal resolution (quarterly surveys) and from a grid of hydrographic stations that poorly described the variability of nearshore waters. These shortcomings together with increasing costs of surveys emphasize the need to establish a coastal site of continuous monitoring to represent the variability of a coastal region in order to generate long-term time-series with higher temporal resolution. The aim of this study is to determine the temporal variability of the physical and chemical properties at a nearshore location, station ENSENADA, with higher frequency sampling, and to demonstrate that this site reflects the main features of the temporal variability (seasonal and interannual) of the coastal waters off Ensenada at northern BC region. The observatory is part of the FLUCAR project ("Carbon sources and sinks in the continental margins of Mexican Pacific waters") and is a site located at an intense coastal upwelling region within a transition zone of the CCS that is strongly influenced by the tropical and subtropical systems.

The paper is organized as follows: first, the historical analysis of 11 years of temperature and salinity data as well as derived geostrophic flows recorded by the IMECOCAL program along a perpendicular transect off Ensenada (BC) is presented. Then, the seasonal variability is contrasted to the temporal characterization of the physical and chemical conditions based on a 2-year data series obtained at higher temporal resolution at the coastal observatory. Finally, the comparison is assessed to consider whether this coastal observatory could be an ocean environmental sensor that is able to perceive the seasonal and interannual variability in the physical and chemical properties of the water column of the coastal waters off Ensenada in the northern BC region. The continuous monitoring of oceanographic conditions of the northeastern Pacific region will not only provide in a more frequent data set for a dynamic region, but will also serve as a framework for future biogeochemical models in the context of global climate change.

2. Material and methods

2.1. Data collection at IMECOCAL line 100

The IMECOCAL sampling grid (Fig. 1, upper panel) occupies the historical CalCOFI lines off BC (Mexico) and extends from Ensenada (31.8°N) to the Gulf of Ulloa (26.5°N). Line 100 located off Ensenada has seven stations (Fig. 1, lower panel) spaced 37 km apart, from the coast (station 30) to 220 km offshore (station 60). During the period 1998–2008, each station along line 100 was sampled seasonally four times a year, usually in January, April, July, and October (Fig. 2). Hydrographic variables in the entire IMECOCAL sampling grid were measured by casts down to 1000 m depth, bottom depth permitting, using a SBE 9/11 CTD, armed with dual temperature and salinity sensors. Data collection and processing procedures as well as details of the IMECOCAL program can be found at http://imecocal.cicese.mx.

2.2. Data collection at station ENSENADA

The FLUCAR project surveys were conducted at station ENSENADA, located south of Punta Banda in Ensenada, BC (31°40.1′N, 116°41.6′W). This coastal site is located ~8 km eastward of IMECOCAL station 100.30 (Fig.1). Eighteen samplings were conducted at this site between October 2006 and November 2008. Routine activities included CTD/rosette casts down to 100 m, with continuous measurements of pressure, temperature, conductivity, and dissolved oxygen (dO_2) using a SeaBird 19 plus CTD. For the inorganic carbon and nutrient measurements, seawater was collected with 5-L Niskin bottles at 10 depth levels with variable spacing during the cruises depending on the depth of the thermocline and the subsurface maximum of chlorophyll. Seawater (500 mL) from the Niskin bottles was collected in Pyrex bottles to determine dissolved inorganic carbon (DIC, the only carbonate system value reported herein). Samples were

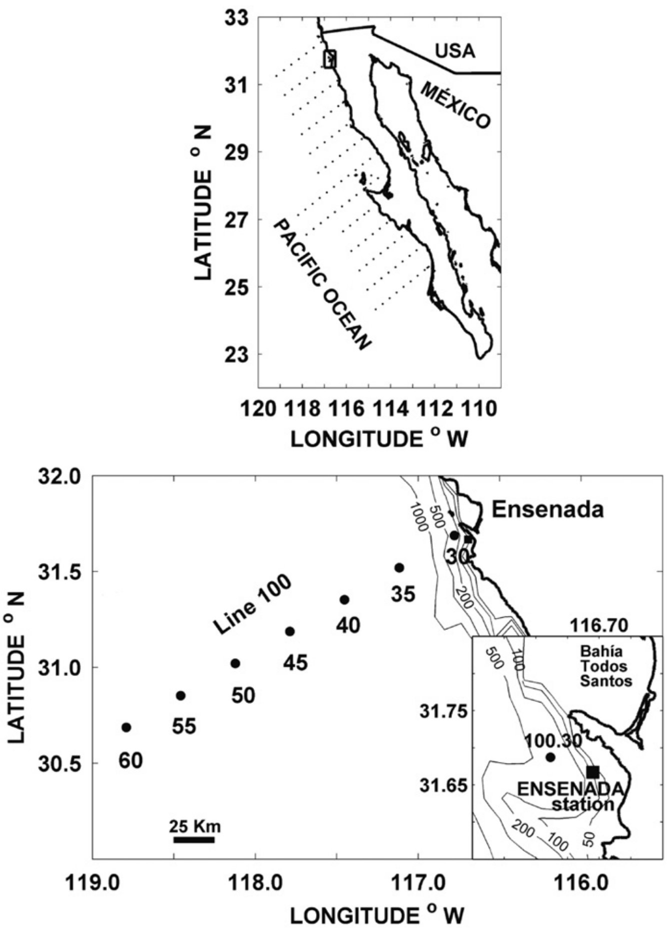

Fig. 1. The IMECOCAL sampling grid (upper panel) and the geographic location of station ENSENADA and the stations of IMECOCAL line 100 (lower panel). Note the proximity of station ENSENADA (8 km) to station 100.30. The 50, 100, 500 and 1000 m isobaths are drawn on the map.

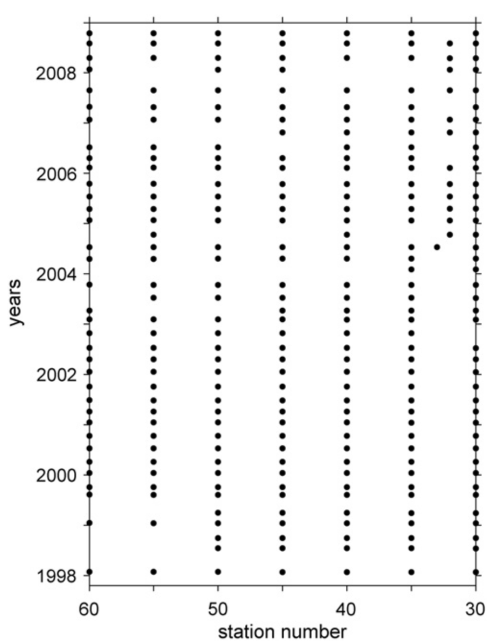

Fig. 2. Station occupation for line 100 used in the harmonic analysis for the period 1998–2008.

immediately poisoned with 100 mL of a saturated HgCl solution to prevent biological alteration, and sealed with Apiezon grease. At the laboratory, DIC was measured by coulometry following the techniques described by DOE (1994). The measuring precision of this procedure was about 1.5 μmol kg^{-1}, whereas the accuracy was approximately 2 μmol kg^{-1}, determined using certified reference material produced by Dr. A. Dickson at Scripps Institution of Oceanography. During each cruise, seawater was also routinely sampled for dO_2 measurements and to calibrate CTD data.

2.3. Data processing

Climatological means of temperature, salinity, and geostrophic velocity were obtained using a harmonic fitting at 12 standard depth levels (0, 10, 20, 30, 50, 75, 100, 125, 150, 200, 250, and 300 m) for all the line 100 stations sampled during the IMECOCAL surveys between 1998 and 2008. The harmonics were calculated following the approach of Lynn (1967) and Chelton (1984), in which the mean seasonal variation is obtained by a least squares regression of the data to annually periodic cosinusoids. The harmonic fitting was restricted to the annual period since the time interval between surveys was 3–4 months. The general form of the harmonic function for the variable $y(t)$ is

$$y(t) = A_0 + A\cos(2\pi\omega t - \varphi)$$

where A_0 is the mean, A and φ are the amplitude and phase of the cosinusoid with frequency ω, and t is the time. The value of A represents half the expected range of variability, while the phase represents the time when the value of $y(t)$ is maximum. Parameters A_0, A, and φ calculated by the fitting were used to obtain estimates of the seasonal means of temperature and salinity for January, April, July, and October.

The variability measured in temperature and salinity vertical distribution pattern at station 100.30 was compared with the hydrographic observations of station ENSENADA obtained over the sampling period (October 2006–November 2008). Chemical data (DIC and dO_2) was also represented for the station ENSENADA during the same sampling period.

Seasonal mean surface and subsurface flow patterns are shown by the cross-section of geostrophic velocity estimations along line 100 for January, April, July, and October. The velocity estimations were computed relative to 400 dbar using the historical hydrographic data of IMECOCAL surveys between 1998 and 2008. The reference level allowed the coastal station (100.30) to be included in the estimates of geostrophic velocity. In order to resolve critical information about slope subsurface currents adjacent to the shelf break, we have included here data from station 100.32, located midway between stations 30 and 35 (Fig. 2).

For the purpose of this work, all data were illustrated by temporal contours between 0 and 300 m depth for the stations of line 100 and between 0 and 95 m depth for the time series of station ENSENADA. Additionally, mean temperature and salinity anomalies of the first 50 m of the water column were calculated for station ENSENADA based on the comparison of the observations done over sampling period October 2006–November 2008 with the seasonal means of temperature and salinity for station 100.30 obtained by the annual fitting to hydrographic data.

Also, to identify interannual variations, monthly upwelling anomalies for 30°N 119°W and bimonthly Multivariate ENSO Indices (MEI, Wolter and Timlin, 1993, 1998) obtained from PFEL-NOAA (http://www.pfeg.noaa.gov/products/PFEL/modeled/indices/upwelling/NA/) and MEI (http://www.esrl.noaa.gov/psd/people/klaus.wolter/MEI/) web pages, respectively, were used for the period sampled at station ENSENADA.

3. Results

3.1. Climatologic analyses of temperature and salinity across line 100

The harmonic fitting parameters resulting from the analysis of line 100 temperature and salinity data are shown in Figs. 3 and 4, respectively. In these figures, density contours of 25.5 and 26.5 kg m^{-3} representing, respectively, the lower limit of CC core (SAW) and the CU core (ESsW) at this latitude (Durazo et al., 2010), are shown. Mean temperature (density) contours in the surface layer (0–100 m, Fig. 3a) show a lifting of the isotherms towards the coast, which indicate that on average the surface flow (CC) is southward, while the downward tilt towards the shore depicted by isolines at larger depths (> 150 m) shows that on average the subsurface flow (CU) is poleward. Steeper slopes are located at the nearshore stations over the continental slope (coastward of station 100.35), associated with coastal upwelling, which seems to be a year-round feature over northern BC coastal waters. The climatological mean of salinity (Fig. 4a) shows the raise of the isohalines towards the coast throughout the water column, with the steeper slopes at the nearshore stations. The CC core ($S < 33.4$) can be observed at approximately 150 km from station 100.30, centered around 50 m depth. The CU signal ($S > 34.2$) is located below 200 m depth at stations close to the coast.

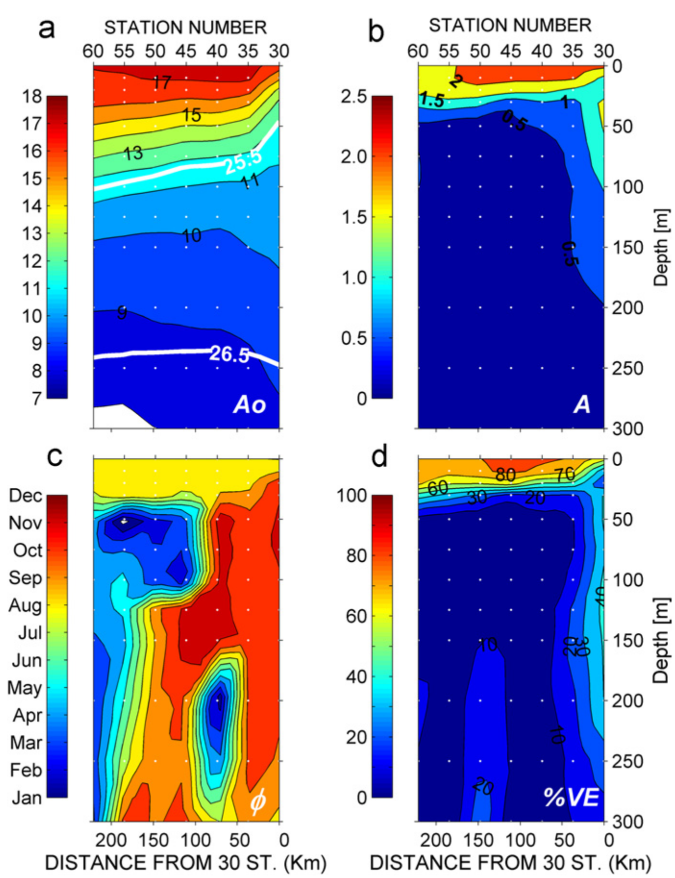

Fig. 3. Climatological temperature (°C) for line 100 generated from 11 years of IMECOCAL data. (a) Mean, (b) amplitude of the annual cycle (°C), (c) phase (months) of the annual cycle that denotes the time in which the cycle is maximum, (d) percentage of explained variance by the annual cycle. The 25.5 and 26.5 kg m^{-3} isopycnal surfaces are indicated by thick white lines, and represent approximations of the lower limit of the CC core (SAW) and the CU core (ESsW), respectively.

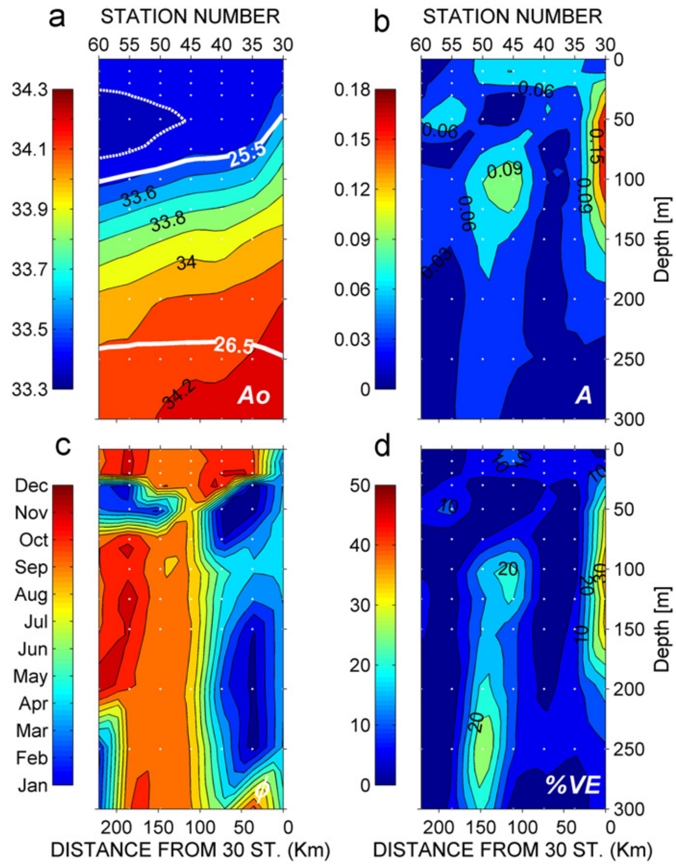

Fig. 4. Climatological salinity contours for line 100 generated from 11 years of IMECOCAL data. (a) Mean, (b) amplitude of the annual cycle, (c) Phase (months) of the annual cycle that denotes the time in which the cycle is maximum, (d) percentage of explained variance by the annual cycle. The 25.5 and 26.5 kg m^{-3} isopycnal surfaces are indicated by thick white lines, and represent approximations of the lower limit of the CC core (SAW) and the CU core (ESsW), respectively.

The seasonal variability, as reflected by the amplitude of the annual signal, is larger than 1.5 °C in the surface layer along the transect and toward nearshore stations (Fig. 3b), associated with the seasonally modulated ocean–atmosphere heat exchange, which warms up/cools down surface waters, and with the seasonal changes of stratification and mixing of the water column due to the variability of the alongshore winds, respectively. Salinity showed larger seasonal amplitude (> 0.10) in a coastal band between 25 and 125 m depth, as well as in a central portion of the transect (Fig. 4b), likely related to seasonal changes in the subsurface flows in this region.

The percentage of explained variance by the harmonic fitting to the temperature signal (Fig. 3d) was typically 60% or larger in the surface layer (~0–25 m). In this surface layer, the phase (Fig. 3c) indicates that the maximum (minimum) temperature occurs in August (February), concurring with solar heating and heat storage cycles, and with coastal upwelling events during the spring transition. Towards the coast there is a second relative maxima in the percentage of explained variance (Fig. 3d) in a narrow band (< 50 km), coincident with the maximum temperature in October (Fig. 3c) linked with subsurface poleward flows. Conversely, the low percentage of explained variance of the surface layer salinity (Fig. 4d) suggests that the variability is mainly due to non-seasonal fluctuations. Though scant seasonal variability in salinity is observed below the surface, relative maxima in the percentage of explained variance (> 20%, Fig. 4d) coincide approximately with the maximum amplitudes of the annual harmonic (Fig. 4b). Phase (Fig. 4c) indicates that saltier waters occur in February–April nearshore and in September–October offshore (>150 km). The time of occurrence of the subsurface coastal core in spring (Figs. 4b and c) suggests a lifting of more saline CU waters in response to wind forcing at the surface. The time of occurrence of the offshore maximum in summer–autumn may indicate the presence or increased advection of CU waters in this portion of transect.

3.2. Seasonal estimates of temperature and salinity for line 100

Harmonic fitting parameters were used to estimate temperature and salinity fields along line 100 for the four seasons of the year, represented in this work by the predicted fields for January, April, July, and October (Fig. 5). The temporal evolution of the hydrographic conditions corroborates that most of the variability in temperature is confined to the first 50 m of depth, with the lowest surface values (<15 °C) during January and the highest (~19 °C) during July. The largest uprising of relatively cold waters (~12 °C) reaching around 25 m depth near the coast is observed in April (Fig. 5, upper panels), associated with the more intense alongshore winds and offshore Ekman transport during spring. The seasonal trend of the vertical distribution of salinity also reveals a peak lifting of coastal waters and stronger cross-shore gradients during spring, although the raise occurs during most of the year. Also, the approach to the coast of a tongue of relative minimum salinity is observed along the transect during April and July (Fig. 5, lower panels) concurrent with the approach to the coast of the offshore CC core and the intensification and maintenance of an equatorward coastal jet in spring and summer, as will be described below (Fig. 6). By autumn, the temperature and salinity contours as well as the 25.5 isopycnal surface depict a more stratified water column. Therefore, low temperature and less saline waters (SAW), which occupy a greater volume of the surface layer (0–100 m depth) across the transect during this season (Fig. 5, Supplementary Fig. 1) are likely associated with the more meandering flow of the CC while

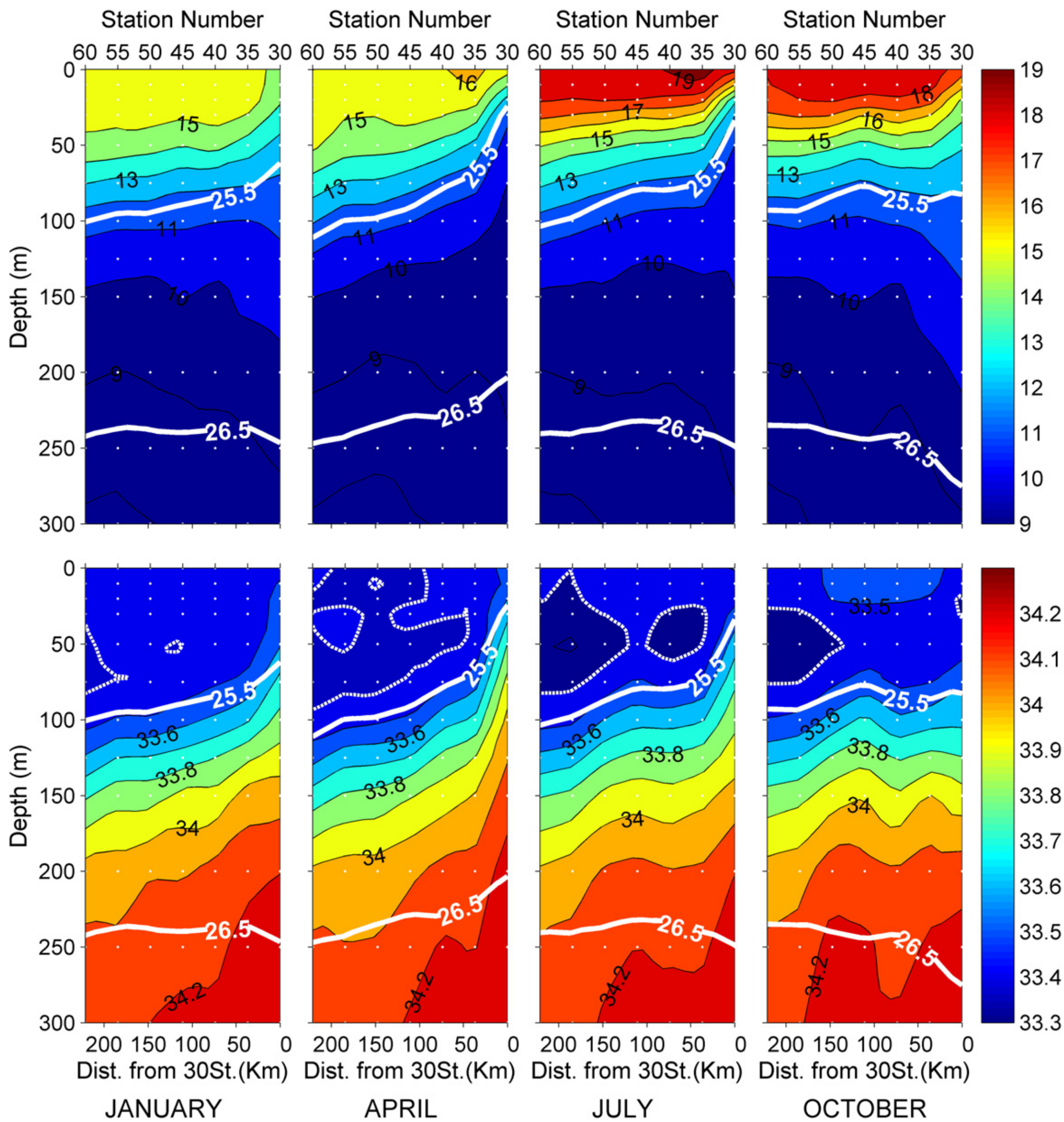

Fig. 5. Temperature (°C, upper panels) and salinity (lower panels) contours for January, April, July, and October across line 100. Values were estimated by harmonic analysis of data collected during 11 years by the IMECOCAL program. The 25.5 and 26.5 kg m^{-3} isopycnal surfaces are indicated by thick white lines and represent approximations of the lower limit of the CC core (SAW) and the CU core (ESsW), respectively.

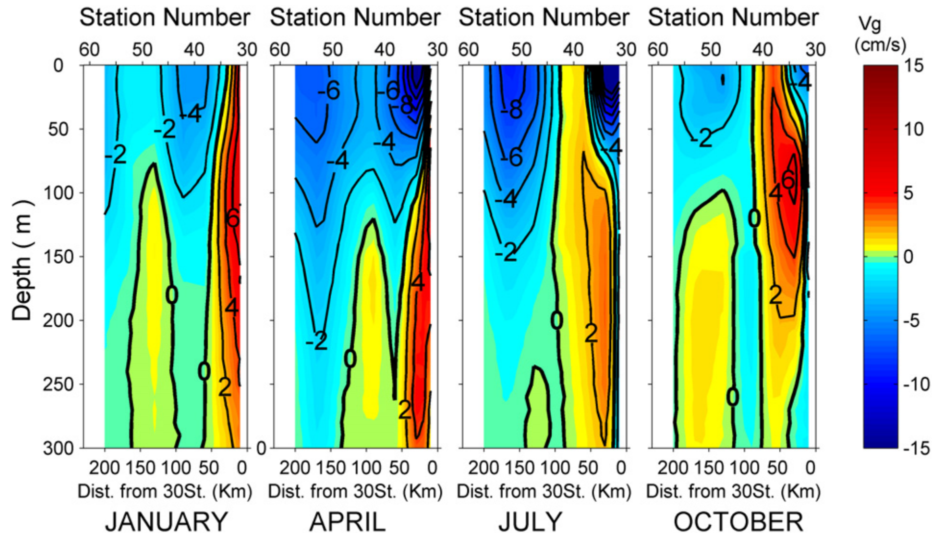

Fig. 6. Cross-sections of geostrophic velocity (cm s^{-1}) for January, April, July, and October across line 100, estimated by harmonic analysis of velocity derived from the hydrographic data collected during 11 years by the IMECOCAL program. The reference level is 400 dbar. Negative (positive) values indicate equatorward (poleward) flows. Contour interval is 2 cm s^{-1}.

passing through northern BC. It is also in this season when near surface (< 100 m depth) isolines and the reduced slope of the 25.5 isopycnal surface evidence a slight downwelling coastward, possibly related with the cyclonic recirculation of CC waters originated by the southward displacement of the Southern California Bight (SCB) eddy (Fig. 5). Mostly during July and October, a slight doming of isolines is observed throughout the water column below 100 m depth and between 100 and 150 km offshore (Fig. 5). This doming could be the result of Ekman pumping manifested as the lifting of more saline subsurface waters originated by the cyclonic circulation in the surface of the CC. Also, as will be shown below, the eastern flank of this dome (< 50 km) appears to be reinforced by the intensification of the poleward flow of the CU, as is indicated by the maximum slope towards the coast of the 26.5 isopycnal surface.

3.3. Seasonal estimates of geostrophic velocity for line 100

Cross-sections of line 100 geostrophic velocity for January, April, July, and October, estimated using the harmonic analysis coefficients (not shown), are depicted in Fig. 6. As indicated by the mean seasonal slopes of isotherms in the previous section, the mean surface flow (< 100 m) depicting the CC is mainly equatorward year-round (negative values), with seasonal variations in its intensity and width across the section (Fig. 6). The equatorward surface flow is divided in two cores, a relatively intense coastal jet that is mainly observed during spring and summer due to the predominance of northwesterly winds favorable to coastal upwelling, and an offshore core associated with the permanent flow of the CC. The coastal jet is also evidenced by the steady lifting of isolines towards the coast during April and July (Fig. 5). Seasonally, the coastal jet is strong (> 10 cm s^{-1}) and occupies the upper 80 m of the water column during April and July, associated with the peak of the upwelling season. In October it appears as a weak flow (~1 cm s^{-1}) next to the coast in the upper 25 m. By January the coastal jet has been displaced offshore (around station 100.40) by an inshore poleward flow (positive values, Fig. 6). In April the coastal jet is wider than in July and it is connected with the offshore CC flow. Although weaker, the same connectivity is observed in January. In contrast, the coastal jet is constrained to shore during July (~50 km) and October (~20 km) and is clearly separated from the offshore CC jet by poleward surface flows (Fig. 6). The offshore CC core exhibits seasonal variability and is located around 150 km from station 100.30, coincident with the low-salinity core (Fig. 4a). It is weaker (~2 cm s^{-1}) and further from shore in January, while during April and July it is stronger (> 6 cm s^{-1}) and closer to the coast. By October, the offshore CC flow weakens (~3–4 cm s^{-1}) and occupies a large part of the offshore waters at the surface layer (0–100 m depth) of the section (Fig. 6), as is evidenced by the greater volume of low temperature and less saline waters (Fig. 5, Supplementary Fig. 1d). Additionally, the presence of poleward surface flows (positive values) seems to be a quasi-permanent feature year-round. The northward surface flow is located in a coastal band that apparently shows cross-section displacement along the year. It is stronger in January and October (> 6 cm s^{-1}), and weaker (< 2 cm s^{-1}) in July. In January, it appears as a narrow flow (< 50 km) next to the coast. By April, it disappears from the upper layers (< 100 m), associated with the intensification of the upwelling winds. In July, this poleward surface current is fully separated from the coast (> 50 km offshore) by the strong equatorward coastal jet, while by October, it flows in a broad band of ~100 km from station 100.30, slightly distant of the shore (Fig. 6). This northward surface flow is apparently the result of the shoaling of the more intense subsurface CU, which is possibly reinforced with the mesoscale activity and cyclonic recirculation of the CC, which in turn is modulated by vertical stratification and a positive wind stress curl nearshore (0–500 km) (Fig. 6).

The mean subsurface flow (> 100 m depth) is mostly poleward (positive values). A main subsurface core is located against the slope year-round and represents the CU. It also shows seasonal variability in its depth and intensity (Fig. 6). The core of the CU is deeper (> 150 m) in April and July, and shallower (~100 m) and more intense (8–10 cm s^{-1}) in January and October. However, the CU is wider (~100 km) in October than in January (< 50 km). Except in April, the slope undercurrent apparently appears connected with poleward surface flows (Fig. 6). Offshore, a less intense subsurface poleward flow (~150 km) co-exists with the slope undercurrent throughout the year although it is more clearly noticeable in October and

January. The offshore core has also been observed off Southern California where it has been suggested that may be the result of a bifurcation of the main core of the CU at deep waters.

3.4. Hydrographic variability for stations 100.30 and ENSENADA

In order to determine whether the hydrographic conditions observed in the coastal observatory (station ENSENADA) reflect the main features of the variability of the coastal region off Ensenada, we compare here the temporal distribution of temperature and salinity of the upper water column (0–100 m) recorded at stations 100.30 and ENSENADA during the period from October 2006 to November 2008. Fig. 7 shows the depth–time evolution of properties, including the 25.5 and 26.2 kg m^{-3} density contours. In general, both stations showed a similar vertical distribution of the hydrographic variables, mainly associated with the seasonal warming/cooling cycles of the surface layer modulated by ocean–atmosphere heat exchange during the sampling period, with the upwelling events of relative saltier and cooler subsurface waters mostly during spring months of 2007 and 2008. For each depth, a statistical comparison (*t*-test) of the hydrographic fields for eight concomitant cruises conducted in both stations revealed that arithmetic means computed were not statistically different ($p < 0.05$), i.e., the null hypothesis (H_0: station 100.30 mean = station ENSENADA mean) was not rejected at each depth level from the surface to 100 m depth. The similarity of temperature and salinity mean profiles between both the stations is evidenced in the Supplementary Fig. 2. Mean and standard errors of these hydrographic variables showed similar variability throughout the water column between both stations. Thus no significant difference between station 100.30 and station ENSENADA was found in the vertical distribution of the hydrographic variables.

Except some particular but, statistically non-significant differences between stations 100.30 and ENSENADA, a marked seasonal pattern was found in the near surface (< 10 m) temperature at both locations. In general, this surface pattern was in agreement with the climatologic seasonal estimates of temperature for line 100 (Fig. 5), though the phase was different in each year. The lowest surface values (< 15 °C) were mostly found during spring 2007 and from winter to spring 2008, while the highest (> 17 °C) during autumn 2006 and from summer to autumn 2007 and 2008 (Fig. 7a and b). In the same surface layer, salinity values showed a

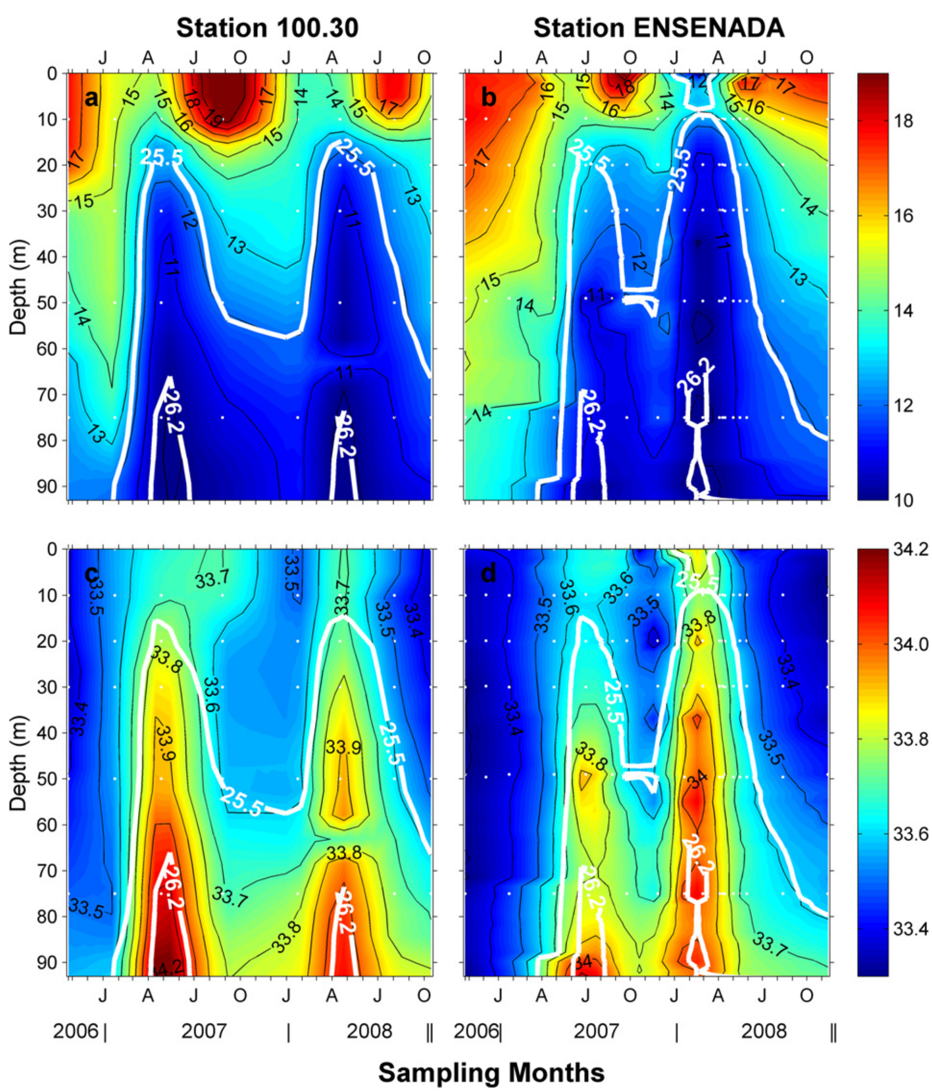

Fig. 7. Temperature (°C) (a, b) and salinity (c, d) contours for station 100.30 and for station ENSENADA of the data collected from October 2006 to November 2008. The 25.5 and 26.2 kg m^{-3} isopycnal surfaces are indicated by thick white lines and represent approximations of the lower limit of the CC core (SAW) and the upper depth limit of the CU (ESsW), respectively. White dots in each plot indicate standard depths.

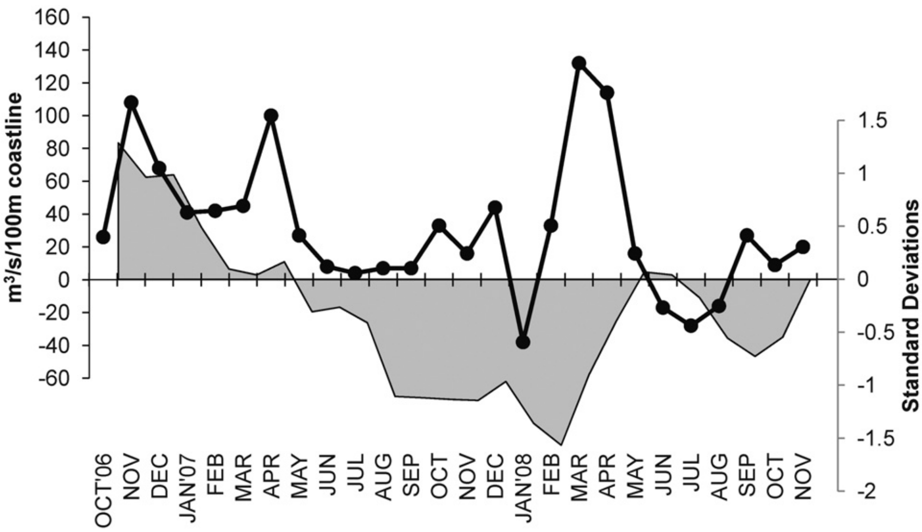

Fig. 8. Monthly upwelling anomalies for 30°N, 119°W (black line-dots) and bimonthly Multivariate ENSO Indices (gray shaded area) for the period October 2006–November 2008. The values of the upwelling index anomaly were obtained from PFEL-NOAA http://www.pfeg.noaa.gov/products/PFEL/modeled/indices/upwelling/NA/, and the MEI index from http://www.cdc.noaa.gov/people/klaus.wolter/MEI/ web pages, respectively.

similar quasi-seasonal pattern (Fig. 7c and d), as was seen in the climatological analyses for line 100 (Fig. 4). Below 10 m depth, a large part of the water column was occupied by cooler (<12 °C) and saltier (>33.8) waters from spring to summer 2007 and also, from winter to spring 2008, likely due to a seasonal lifting of isolines caused by wind-driven vertical pumping at the surface, as was indicated by the appearance of the 26.2 kg m^{-3} isopycnal surface at shallower depths at both stations (Fig. 7c and d). From the sampling period, the upwelling observed during 2008 was more intense than for 2007, as was evidenced by the more saline waters ($\sim$33.7) that reached the surface during spring 2008 (Fig. 7c and d). This interannual variation is likely associated with environmental indices related with the intensity of upwelling (Coastal Upwelling Index Anomaly) and the large-scale ocean–atmosphere variability (MEI) (Fig. 8). The surfacing of the relatively salty waters during 2008 was likely associated with an intensification of upwelling events (positive upwelling anomalies) during a cold ENSO phase, i.e. La Niña condition, represented by negative MEI values from summer 2007 to spring 2008 (Fig. 8).

3.5. Temperature and salinity anomalies for station ENSENADA

Harmonic fitting to temperature and salinity data for line 100 showed that their largest fluctuations occur in the first 50 m of the water column (Figs. 3 and 4). Given the fact that temporal variability of properties at station ENSENADA resembles that of station 100.30 (Fig. 7), mean temperature and salinity anomalies of the upper 50 m of the water column were calculated for station ENSENADA (Fig. 9) with respect to the corresponding climatological means obtained for station 100.30 (Figs. 3a and 4a). The temporal evolution showed positive temperature anomalies of $\sim$1 °C at the end of 2006 and beginning of 2007 (Fig. 9a). These anomalies coincided with the higher than normal temperature values recorded above 50 m during winter of 2006 (Fig. 7b) and also at station 100.30 (Fig. 7a). This positive temperature anomaly coincided with the positive MEI values recorded from October 2006 to February 2007 as indicative of the warm ENSO phase, i.e., El Niño condition (Fig. 8). Except the slight positive anomaly observed in August 2007, surface waters were colder than the climatological average from January 2007 to the end of 2008. Maximum negative values were observed between autumn 2007 and spring 2008 (Fig. 9a), which coincided with negative MEI values (La Niña condition) from May–June 2007 to April–May 2008 (Fig. 8). Associated with these large-scale conditions, the region also experienced stronger than normal upwelling during February–April 2008 as was indicated by the upwelling index anomaly for 30°N. Thus, the anomalous conditions observed in spring 2008 were originated by large-scale events that modulated local forcings.

Concomitant with the advection of saltier waters from the south during El Niño and increased upwelling and offshore Ekman transport during La Niña, due to stronger than normal alongshore winds occurring during these cold events, salinity anomalies were positive throughout the sampling period, with larger magnitude during spring of both 2007 and 2008 (Fig. 9b). Maximum values were recorded in spring 2008, and similar to the temperature anomalies, the saltier than normal waters at station ENSENADA were likely caused by an upwelling intensification of subsurface waters under La Niña cold conditions (Fig. 8).

3.6. Distribution of chemical variables for station ENSENADA

The temporal distribution of chemical variables at the coastal station (Fig. 10) showed a similar pattern to that depicted by the thermohaline properties (Fig. 7). Although the highest concentrations of dO_2 depicted a trend occurring at the surface due to the larger ocean–atmosphere exchange, the presence of less saline (Fig. 7d) and well-oxygenated waters (>300 μM) throughout the water column was notable from the end of 2006 to the beginning of 2007 (Fig. 10a). Thus, the prevailing water mass during this period was of subarctic origin (SAW), likely associated with a deeper seasonal thermocline due to El Niño conditions recorded in this period (Fig. 8). Also, the spring seasons of 2007 and 2008 were characterized by a lifting of low dO_2 waters, likely associated with the penetration into the surface layer of waters carried by the CU from the equatorial region. As shown before, this lifting during spring 2008 was very intense, so colder, saltier waters with dO_2 concentrations <150 μM were recorded close to the surface at this coastal observatory (Fig. 10a).

The temporal distribution of DIC throughout the water column showed the highest values associated with deeper waters (Fig. 10b). Worth noting were the low surface values and the lifting of DIC-rich subsurface waters in the spring of both 2007

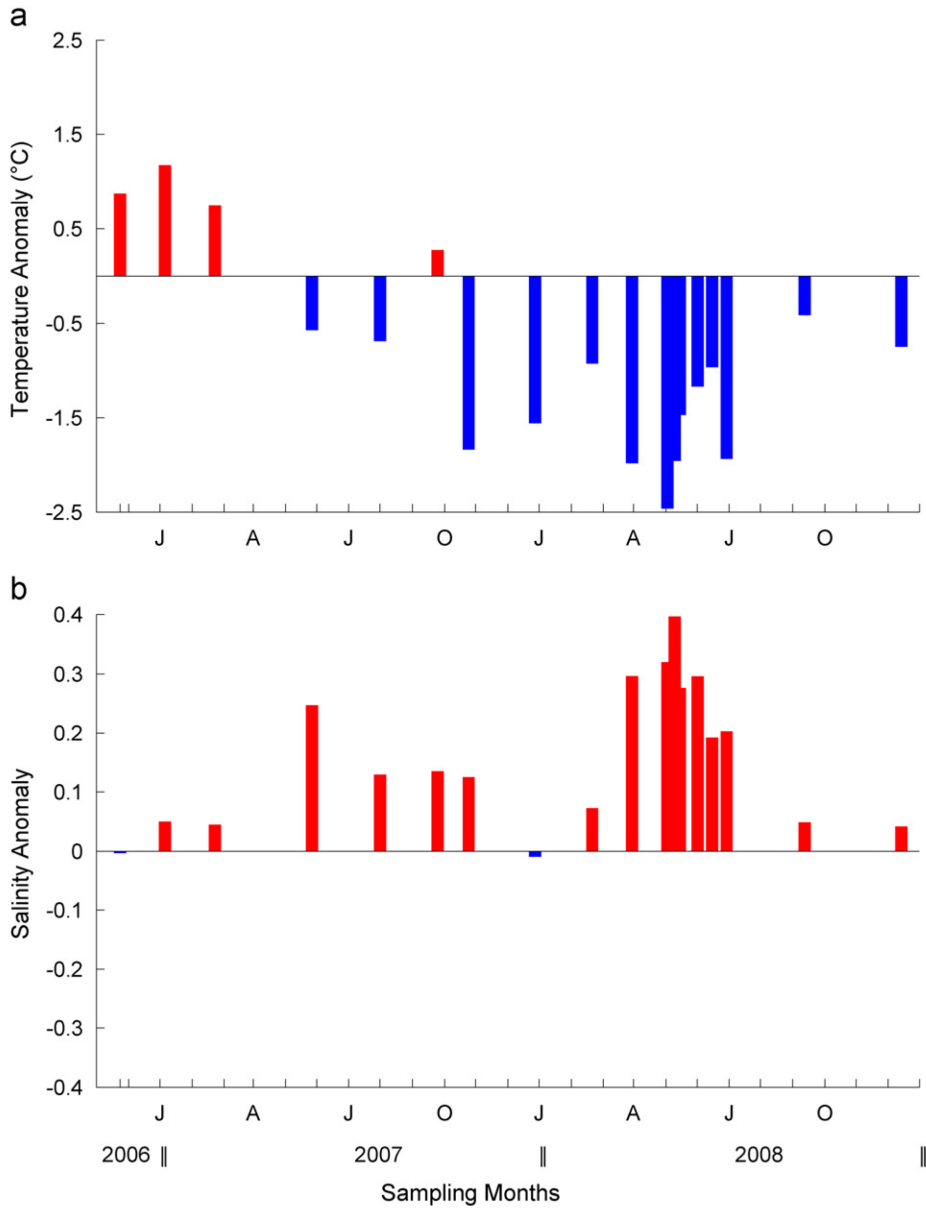

Fig. 9. Mean (a) temperature (°C) and (b) salinity anomalies of the upper 50 m of the water column for the data collected at station ENSENADA from October 2006 to November 2008. Anomalies were computed relative to the climatological means obtained for station 100.30 by the annual fitting to hydrographic data.

and 2008. Concomitant with the behavior of the hydrographic variables, the shoaling of DIC isolines was more pronounced during spring 2008, with maximum values of ~2165 μmol kg^{-1} at a scant 30 m depth. As a macronutrient, DIC presented a similar behavior to that of micronutrients such as nitrate, phosphate, and silicate (data contours not shown). The highest DIC concentrations at shallower depths in April 2008 were associated with the physical characteristics (salty and cold) of the water mass (ESsW) upwelled from subsurface towards surface layers.

4. Discussion

The analysis of the historical hydrographic measurements (1998–2008) at coastal waters off Ensenada presented above illustrates a marked seasonal variability in the physical and chemical conditions. Greatest temperature variability occurred in the surface layer close to the coast (< 100 m, Fig. 3) modulated by seasonal fluctuations in air–sea exchanges, as well as wind variability that controls coastal upwelling, stratification, and surface circulation patterns. The seasonal variability in salinity was found weaker at the surface and stronger toward subsurface layers (Fig. 4), associated with the seasonality of the coastal upwelling and the structure of surface and subsurface flows. Thus, a large part of the variability in the hydrographic conditions off Ensenada is due to the seasonal fluctuations of the strength of the circulation and the variability in the characteristics of water masses feeding into the surface and subsurface flows.

Along the transect analyzed, it was found that the core of the CC that transports equatorward relatively low-salinity water of subarctic origin was located further away from the coast (~200 km) during winter, but closest to shore (~100 km) during spring–summer (Figs. 5 and 6). The proximity to the coast of the mean position of this offshore CC core during spring–summer was also observed in the region of Southern California Bight (SCB) (Bograd and Lynn, 2003), and has been associated with the

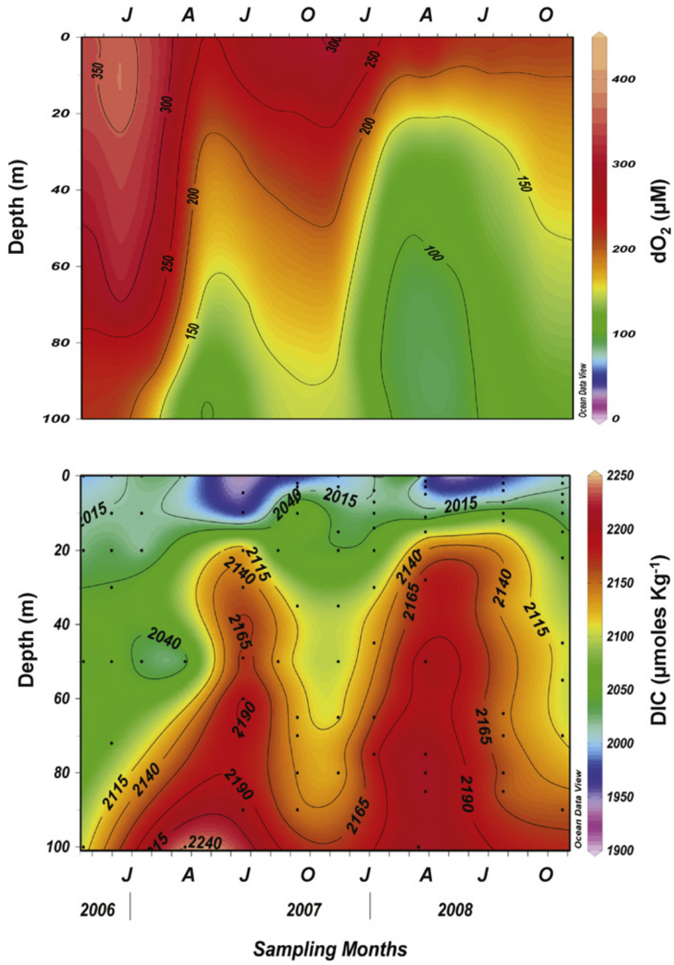

Fig. 10. Contours of concentration of (a) dissolved oxygen (μM) and (b) dissolved inorganic carbon (μmol kg^{-1}) for the data collected at station ENSENADA from October 2006 to November 2008.

springtime development of a coastal equatorward jet (Lynn et al., 2003). The southward flow near to the coast was also recorded in this work, being more intense (>10 cm s^{-1}) during spring and summer (Fig. 6). Since this coastal jet is not associated with the relative minimum of near surface salinity offshore, we suggest that it is made of a mixture of subarctic CC water and more salty subsurface water eroded from the upper CU during strong upwelling events. This finding is supported by the seasonal mean *T* and *S* diagrams for April (Supplementary Fig. 1b) when more saline waters from subsurface layers (ESsW) are evidenced mostly at station 100.30 compared to other stations of the section. This is in agreement with observations conducted further north in the CCS (Hickey, 1979; Lynn and Simpson, 1987; Bograd and Lynn, 2003), although in those regions the coastal jet reverses direction in response to local forcing. The seasonality of the southward coastal flow may be explained in terms of a geostrophic adjustment to coastal upwelling. The alongshore winds are stronger during spring–summer (Pérez-Brunius et al., 2007) and bring to the surface cooler and saltier waters, generating maximum vertical and horizontal gradients of the upper 200 m. This is also seen in the results of the harmonic fitting of salinity (and harmonic fitting of velocity, not shown), which represent a relatively large proportion of the explained variance near the coast with the maximum signal during spring (Fig. 4).

Poleward surface flows were evidenced close to the coast (within the first 100 km from station 100.30) during summer, autumn, and winter (Fig. 6). Previous studies that used current meter moorings in three nominal depths (25, 42 and 60 m) on the continental shelf off Ensenada in the period 1978–1979 (Barton, 1985) demonstrated that flows were northward year-round below 25 m depth, and at all levels only in the period from May to October. Furthermore, Alvarez et al. (1984, 1990) reported surface coastal poleward flows related to weak wind conditions for two coastal sites located at 31.3°N and 32.5°N. Frequently, surface geostrophic flows have been associated with small-scale (20–50 km) cyclonic circulation regions produced by strong upwelling near capes and coastal promontories off BC (Durazo and Baumgartner, 2002; Durazo et al., 2005). More recently, 10 years of ship-borne ADCP measurements analyzed by Gay and Chereskin (2009) demonstrated that coastal poleward surface flows (above 100 m depth) occur inside the SCB slightly separated from the coast by equatorward currents during summer, autumn, and winter. In a regional context, Lynn and Simpson (1987) showed that south of Point Conception (34.5°N), the equatorward CC flows offshore ($\sim$500 km) and divides in two branches at the latitude of Ensenada, one that impinges on the coast near Punta Baja (29°N) and another that flows coastward to become the SCB eddy. They demonstrated that the eddy shows a clear seasonal variability in strength and position, with its southernmost location during summer–autumn. These previous findings suggest that July, October, and even January surface poleward coastal flows presented here form part of the eastern limb of the SCB eddy that extends southward over the northern BC region.

The summer, autumn, and winter processes described here seem to be related with wind stress patterns along the coast and the latitudinal displacement of the SCB eddy. As spring transitions to summer–autumn, upwelling winds relax close to the coast, but remain strong further offshore the continental slope, generating a positive wind-stress curl (cyclonic). This positive curl has been associated with the recirculation of CC waters in the SCB region (Di Lorenzo, 2003). Moreover, positive wind stress curl has been reported for northern BC (30°N) by Castro and Martínez (2010), linked to the wind patterns in the SCB region. Such positive wind-stress curl is a physical mechanism that generates Ekman pumping of more saline, poor in dO_2 and nutrient-rich subsurface waters to upper levels, particularly downstream coastal prominences (Bakun and Nelson 1991, Chelton et al., 2004; Rykaczewski and Checkley, 2008). Off Ensenada, evidence of this forcing is seen by the doming structure observed in July and mostly in October (Fig. 5), a feature that extends vertically throughout the water column in the central part of line 100. The seasonality of this "lifting" was made evident in the relatively large explained variance near 200 m depth shown by the harmonic fitting to salinity (Fig. 3d), which has its maximum value around October. Thus, the dome structure observed in our region in July and October is likely due to the pumping of more saline subsurface waters toward upper depth levels (Fig. 5) and would be the subsurface signature of the southward extension of the surface circulation related to the SCB eddy (Fig. 6).

Subsurface flows were identified year-round mainly by the CU flow located over the continental slope and by a weaker secondary core $\sim$150 km offshore (Fig. 6). Their presence in our zone confirms the general feature of the eastern boundary current systems, which has a clear seasonal variability. Hydrographic fields illustrated a downward tilt towards shore of the 26.5 isopycnal surface during most of the year, the approximation of CU core against the slope in our region (Fig. 5). Similarly, the seasonal mean *T*–*S* diagrams for line 100 (Supplementary Fig. 1) shows the presence of ESsW (transported by the CU) during all year, especially toward the most coastal stations. The poleward subsurface flows were also reflected in the mean seasonal geostrophic velocity contours, being the slope undercurrent stronger (>8–10 cm s^{-1}) and shallower ($\sim$100 m) in autumn and winter compared with summer when it was found to be weak ($<2\ \mathrm{cm\,s^{-1}}$) below 100 m depth. Excepting spring, when the slope undercurrent occurred deeper (below 150 m depth) in a band constrained to the coast, the CU seems to be connected with poleward surface flows the rest of the year. The couplings with northward surface flows have also been recorded for waters off southern California, where the CU was found more intense both in summer and autumn, especially inside the SCB (Gay and Chereskin, 2009). The secondary core has also been documented for Southern California where it has been suggested that the offshore subsurface poleward current results from a bifurcation of the main CU off San Diego, and that such bifurcation converge near Point Conception. Our data indicate that the two cores co-exist off Ensenada. At present, the origin of the secondary offshore subsurface poleward current remains unclear. Subsurface currents along the Baja California peninsula (not shown) suggest a pattern similar to Southern California, with a core south of Punta Eugenia and two cores elsewhere. It has been suggested (Holloway, 1992) that the interaction of mesoscale eddies with bottom topography may have some influence on the generation, width or location of undercurrents near the continental slope. Such subsurface structures are common along the CCS (Garfield et al., 1999; Jeronimo and Gómez-Valdés, 2007). It is thus likely that poleward subsurface flows become well organized before reaching coastal prominences, and that the bifurcation to be generated downcurrent. However, more studies are needed to understand the underlying mechanisms that favor the splitting of the main CU in two branches.

In a regional context, subsurface geostrophic flows (200/500 dbar) off northern BC ($>28^{\circ}$N) are characterized by a cyclonic circulation, a deep signature of the SCB eddy (Durazo, 2009). The position and size of this subsurface cyclonic circulation exhibit seasonal variability, being absent or diffuse during spring and better defined during summer and autumn (Durazo et al., 2010). Since the seasonality of this cyclonic circulation concurs mainly in autumn with the variability of the slope CU flow described here, it is feasible that coastal poleward subsurface flows across line 100 may be identified as the eastern limb of the subsurface cyclonic gyre. Therefore, the seasonal intensification and shoaling of the slope undercurrent, as well as the bifurcation from the main CU core (offshore CU) could be seasonally reinforced by the strengthening and southward extension of the SCB eddy, considered here as a deeper expression of the surface cyclonic recirculation of the CC over northern BC waters.

The higher temporal resolution data set shown for station ENSENADA, located only 8 km eastward of station 100.30 (the closest station to line 100), revealed that this site is capable of perceiving the seasonal variability in the physical and chemical properties of the water column for the coastal region off Ensenada [$<$ 50 km, the local decorrelation scale, Walstad et al., 1991; Denman and Freeland, 1985], and also to some seasonal circulation patterns that have been described above. Consistent with observations for station 100.30, station ENSENADA showed larger surface heating in the summer modulated by seasonal fluctuations in air–sea exchanges, a larger input of cold, saline waters in the surface layer associated with coastal upwelling in spring–summer, and the presence of relatively low-salinity waters in most of the surface layer (<50 m) in autumn–winter (Figs. 7c and 7d). Although station 100.30 is deeper (<500 m) than station ENSENADA ($\sim$100 m), the intensification of poleward flows (CU) during autumn–early winter was practically undetectable at either location. Instead, in spring–summer an equatorward coastal jet characterized by salty waters in comparison to the CC core (Fig. 7b) seems to be more related with the erosion of subsurface waters lifted to shallower depths by vertical Ekman transport produced by the year-round alongshore winds, which are more intense and persistent in spring (Bakun and Nelson, 1977; Huyer, 1983; Pérez-Brunius et al., 2007). Thus, persistent coastal upwelling driven by alongshore winds may be an important physical mechanism for the input of subsurface waters towards the coast in this region, mainly during spring–summer.

Our findings indicate that station ENSENADA is also a site sensitive to interannual signals (Fig. 7c and d) as was reflected by the mean positive temperature anomalies ($\sim$1 °C; Fig. 9a) recorded during El Niño conditions (Goericke et al., 2007; Durazo, 2009) from late 2006 to the beginning of 2007. This warming was also observed in the positive MEI values recorded by the end of 2006 (Fig. 8). Although positive salinity anomalies were also recorded at station ENSENADA, the values were low (<0.1) in comparison with those recorded in subsequent months (Fig. 9b). This may be because the poleward surface advection of waters of tropical and subtropical origin that has been associated with this type of events off BC (Durazo and Baumgartner, 2002) occurred as a tongue of relatively more saline water that only extended to latitudes close to 29°N (Goericke et al., 2007; Durazo, 2009). Towards early 2007, El Niño conditions quickly disappeared in the CCS giving way to La Niña, which continued until early summer 2008 (McClatchie et al., 2008; Durazo, 2009), as it was indicated by the Oceanic NINO Index reported by the NOAA Climate Prediction Center (http://www.cpc.noaa.gov/) for the period December 2007–January/February 2008, as well as by the negative values of MEI Index from May/June 2007 to April/May 2008 (Fig. 8). During this same period, the Pacific Decadal Oscillation (PDO) Index was negative for the North Pacific due to negative anomalies in sea surface temperature, with colder than usual temperatures in the CC and the Gulf of Alaska (McClatchie et al., 2008). Further, the upwelling favorable winds were more intense than normal off the coasts of central California and BC in spring 2007 and 2008 (Goericke et al., 2007; McClatchie et al., 2008). The upwelling index anomalies data reported by NOAA for 30°N reported high index values in the spring of both 2007 and 2008, with maximum positive anomalies ($>100\ \mathrm{m^3\,s^{-1}}$ per 100 m of coastline) in March and April 2008 (Fig. 8). This concurs with the notable lifting of cold, more saline subsurface waters, poor in dO_2 and rich in nutrients, observed at station ENSENADA from February to June 2008 (Figs. 7c and d and 10). As a consequence, the interannual variability observed in the thermohaline conditions at this coastal location may be linked to ENSO events with effects in the warming (El Niño) or cooling (La Niña) of local waters that generated anomalies in the regional flows and in the intensity of coastal upwelling. At these interannual timescales, the upper mixed layer also exhibits variability in temperature and salinity for the waters along the BC Peninsula, associated mainly with regional (northern and southern BC) differences in the atmosphere–ocean net heat fluxes and with large-scale variability in the sea surface height anomaly, respectively (Gómez-Valdés and Jeronimo, 2009). Thus, it is likely that at longer timescales the signal of large-scale (PDO) variability would be also detected in a shallow coastal region as station ENSENADA.

Changes in hydrographic properties are very important for marine ecosystems. In particular, seasonal and long-term variations in the physical and chemical water properties can cause alterations in the structure of the water column, such as in mixed layer and thermocline depths, and the strength of vertical stratification. Therefore, fluctuations of properties in the water column can generate changes in the input of inorganic nutrients to the euphotic zone, with the consequent impact on primary and secondary production (Lavaniegos and Ohman, 2003; Gaxiola-Castro et al., 2008). In the long-term, these changes could become evident at station ENSENADA that is modulated by seasonal and interannual variability. Particularly during spring 2008, the fluctuations in the hydrographic variables were associated with the intensified upwelling of subsurface waters that were poor in dO_2, but rich in DIC and nutrients, into the euphotic zone (Fig. 10). Enhanced advection of low-pH subsurface waters, rich in DIC and subsaturated in aragonite, onto the continental shelf, can seriously affect marine organisms that form calcareous shells and skeletons. In fact, recent results have shown that upwelling plays an important role in the transport of waters affected by the acidification of the ocean over the continental shelf of North America (Feely et al., 2008). Likewise, an increased input of poor dO_2 waters into surface layers caused by seasonal upwelling can result in severe ecological impacts on the ecosystem, especially in areas where the continental shelf is close to hypoxic conditions. For example, in coastal waters off southern California, a decrease in dO_2 as well as an increase in the hypoxic limit ($\sim$60 μmol/kg) above 90 m depth have been recorded in the surface layer at 100 m depth over a period of 23 years, mainly along the continental shelf and break (Bograd et al., 2008). An expansion in the water column of the oxygen minimum layer could lead to cascading effects on benthic and pelagic ecosystems, including habitat compression and community reorganization (Bograd et al., 2008; Chan et al., 2008). Thus, monitoring the oceanographic conditions at a coastal station in the northeastern Pacific not only provides a more frequent data set for this dynamic region, but also generates an environmental framework to evaluate the variability in the coastal waters at different timescales (seasonal, interannual, decadal) of this part of the CCS, as well as to define a baseline for future biogeochemical models in the context of global climate change.

5. Conclusions

The results of the historical analysis of hydrographic data gathered at coastal waters off Ensenada, BC, revealed a marked seasonal variability in the physical and chemical conditions of the northern BC region. It was found that temperature variability occurs mainly in nearshore surface layers ($<$100 m), while salinity variability increases towards subsurface layers. The variability described in both parameters is modulated by seasonal fluctuations in air–sea exchanges and also by wind patterns (alongshore and cyclonic wind-stress curl) that control coastal upwelling, stratification of the water column, and surface (CC) and subsurface (CU) seasonal circulation patterns. During spring–summer, the main physical process that modifies the nearshore hydrographic conditions is coastal upwelling driven by strong alongshore winds, which results in the presence of relatively more saline, cooler, poor in dO_2 and nutrient-rich subsurface waters and the intensification of an equatorward surface coastal jet. It was also found that a large part of the variability during summer–autumn and winter represents the main features of the seasonality of circulation patterns off southern California and northern BC, namely: (1) the southward extension of the SCB eddy with an intense mesoscale activity, (2) the surface poleward flows in a narrow coastal band ($<$100 km) and below this, the subsurface poleward flows of the CU, both linked to the CC cyclonic recirculation and the permanent northern subsurface cyclonic eddy, (3) the offshore bifurcation of the main CU core located against the slope, (4) the upward intrusion of more saline subsurface waters by Ekman pumping (positive wind-stress curl), and (5) the intensification of the slope undercurrent.

Particularly, the seasonal variability observed at station ENSENADA, a coastal monitoring observatory, was similar to that described for station 100.30, and reflects adequately the seasonal variability of the coastal waters ($<$50 km) off Ensenada, BC. In addition to this seasonal variability, the coastal site reflected the interannual variability associated with warm and/or cold basin-wide events that modified the water column structure in this coastal region. This was evidenced in station ENSENADA by the negative temperature (~ -1.5 °C) and positive salinity ($\sim$0.3) anomalies recorded in spring 2008, when subsurface waters of equatorial origin poor in dO_2 and rich in DIC were found at 30 m depth due to the intensification of coastal upwelling events at this time of year. This coincided with high positive anomalies of the upwelling index ($>$100 $m^3\,s^{-1}$ per 100 m of coastline) reported by NOAA in March and April 2008 at 30°N, and with an increase in wind intensity off central California and BC in spring 2008, all related to the La Niña event indicated by the MEI index from the summer 2007 to mid 2008. Thus, station ENSENADA would be a good site to monitor the oceanographic conditions of coastal waters of the northern BC region, an area that not only is located within a transition zone of the CCS strongly influenced by subarctic waters from the north, and tropical and subtropical systems from the south, but also is part of a major eastern boundary current system where upwelling controls the structure of the water column and ecosystems.

Acknowledgments

The IMECOCAL program has been mainly funded by CONACYT (projects G0041T, G35326T, 017PÑ-1297, C02-42569, 47044, 48367, and 23947), SEMARNAT-CONACYT (23804), and UC-MEXUS (CN07-125), as well as by UABC (323 and 341). The FLUCAR project was supported by CONACYT (SEP-2004-C01-45813/A-1) and the project entitled "Studies of parameters of the CO_2 system in coastal Pacific waters" by CONACYT (25339). We thank the crew of the R/V *Francisco de Ulloa* for the time and effort dedicated during all the cruises, as well as the crew of the skiff boat *GENUS* for their initiative and collaboration. Special thanks to the CICESE and UABC students, technicians, and researchers whose work was crucial for the success of the IMECOCAL and FLUCAR programs. We are also grateful to the two anonymous reviewers for their valuable comments that greatly improve this work.

Appendix A. Supplementary material

Supplementary data associated with this article can be found in the online version at doi:10.1016/j.csr.2010.07.011.

References

Alvarez, L.G., Durazo, R., Pérez, J., Navarro, L.F., Hernández, R., 1984. Observaciones de corrientes costeras superficiales mediante trazadores Lagrangeanos II. Eréndira, Baja California, 1979–1981. Unpublished Report, Departamento de Oceanografía Física, Centro de Investigación Científica y de Educación Superior de Ensenada, Ensenada, México (in Spanish).

Alvarez, L.G., Godínez, V.M., Lavín, M.F., 1990. Near-shore dispersion off Tijuana, Baja California. Ciencias Marinas 16, 87–109.

Bakun, A., Nelson, C.S., 1977. Climatology of upwelling related processes off Baja California. California Cooperative Oceanic Fisheries Investigation Reports 19, 107–127.

Bakun, A., Nelson, C.S., 1991. The seasonal cycle of wind-stress curl in subtropical eastern boundary current regions. Journal of Physical Oceanography 21, 1815–1834.

Barton, E.D., 1985. Low-frequency variability of currents and temperatures on the Pacific continental shelf off northern Baja California, 1978 to 1979. Continental Shelf Research 4, 425–443.

Barton, E.D., Argote, M.L., 1980. Hydrographic variability in an upwelling area off Northern Baja California in June, 1976. Journal of Marine Research 38, 631–649.

Bograd, S.J., Lynn, R.J., 2003. Long-term variability in the southern California Current System. Deep Sea Research Part II 50, 2355–2370.

Bograd, S.J., Castro, C.G., DiLorenzo, E., Palacios, D., Bailey, H., Gilly, W., Chavez, F.P., 2008. Oxygen declines and the shoaling of the hypoxic boundary in the California current. Geophysical Research Letters 35, L12607. doi:10.1029/2008GL034185.
Castro, R., Martínez, A., 2010. Variabilidad espacial y temporal del campo de viento frente a la península de Baja California. In: Durazo, R., Gaxiola, G. (Eds.), Dinámica del Ecosistema Pelágico frente a Baja California, 1997-2007: Diez Años de Investigaciones Mexicanas de la Corriente de California. Instituto Nacional de Ecología (INE)/ Centro de Investigación Científica y de Educación Superior (CICESE), México (in Spanish).
Chan, F., Barth, J.A., Lubchenco, J., Kirincich, A., Weeks, H., Peterson, W.T., Menge, B.A., 2008. Emergence of anoxia in the California current large marine ecosystem. Science 319, 920.
Chelton, D.B., 1984. Seasonal variability of alongshore geostrophic velocity off central California. Journal of Geophysical Research 89 (C3), 3473–3486.
Chelton, D.B., Schlax, M.G., Freilich, M.H., Milliff, R.F., 2004. Satellite measurements reveal persistent small-scale features in ocean winds. Science 303, 978–983.
Denman, K.L., Freeland, H.J., 1985. Correlation scales, objective mapping, and a statistical test of geostrophy over the continental shelf. Journal of Marine Research 43, 517–539.
Di Lorenzo, E., 2003. Seasonal dynamics of the surface circulation in the Southern California current system. Deep Sea Research Part II 50, 2371–2388.
DOE, 1994. Handbook of methods for the analysis of the various parameters of the carbon dioxide system in sea water. In: Dickson, A.G., Goyet, C. (Eds.), Version 2. ORNL/CDIAC-74.
Durazo, R., Baumgartner, T., 2002. Evolution of oceanographic conditions off Baja California: 1997–1999. Progress in Oceanography 54, 7–31.
Durazo, R., Gaxiola-Castro, G., Lavaniegos, B., Castro-Valdez, R., Gomez-Valdes, J., Mascarenhas Jr., A.S., 2005. Oceanographic conditions west of baja California, 2002–2003: a weak El Niño and subartic water enhancement. Ciencias Marinas 31, 537–552.
Durazo, R., 2009. Climate and upper ocean variability off Baja California, Mexico: 1997–2008. Progress in Oceanography, doi:10.1016/j.pocean.2009.07.043.
Durazo, R., Ramírez, A.M., Miranda, L.E., Soto-Mardones, L.A., 2010. Climatología hidrográfica de la Corriente de California frente a Baja California. In: Durazo, R., Gaxiola, G. (Eds.), Dinámica del Ecosistema Pelágico frente a Baja California, 1997–2007: Diez Años de Investigaciones Mexicanas de la Corriente de California. Instituto Nacional de Ecología (INE)/ Centro de Investigación Científica y de Educación Superior (CICESE), México (in Spanish).
Feely, R.A., Sabine, C.L., Hernandez-Ayón, J.M., Ianson, D., Hales, B., 2008. Evidence for upwelling of corrosive "acidified" water onto the continental shelf. Science 320, 1490. doi:10.1126/science.1155676.
Gay, P.S., Chereskin, T.K., 2009. Mean structure and seasonal variability of the poleward undercurrent off southern California. Journal of Geophysical Research 114, C02007. doi:10.1029/2008JC004886.
Gaxiola-Castro, G., Durazo, R., Lavaniegos, B., De la Cruz-Orozco, M.E., Millán-Nuñez, E., Soto-Mardones, L., Cepeda-Morales, J., 2008. Pelagic ecosystem response to interannual variability off Baja California. Ciencias Marinas 34, 263–270.
Goericke, R., Venrick, E., Koslow, T., Sydeman, W.J., Schwing, F.B., Bograd, S.J., Peterson, W.T., Emmett, R., Lara-Lara, J.R., Gaxiola-Castro, G., Gómez-Valdés, J., Hyrenbach, K.D., Bradley, R.W., Wiese, M.J., Harvey, J.T., Collins, C., Lo, N.C.H., 2007. The state of the California current, 2006–2007: regional and local processes dominate. California Cooperative Oceanic Fisheries Investigation Reports 48, 33–66.
Garfield, N., Collins, C.A., Paquette, R.G., Carter, E., 1999. Lagrangian exploration of the California Undercurrent, 1992–95. Journal Physical Oceanography 29, 560–583.
Gómez-Valdés, J., Jeronimo, G., 2009. Upper mixed layer temperature and salinity variability in the tropical boundary of the California current, 1997–2007. Journal of Geophysical Research 114, C03012. doi:10.1029/2008JC004793.
Hickey, B.M., 1979. The California current system, hypotheses and facts. Progress in Oceanography 8, 191–279.
Holloway, G., 1992. Representing topographic stress for large-scale ocean models. Journal Physical Oceanography 22, 1033–1046.
Huyer, A., 1983. Coastal upwelling in the California current system. Progress in Oceanography 12, 259–284.
Jeronimo, G., Gómez-Valdés, J., 2007. A subsurface warm-eddy off northern Baja California in July 2004. Geophysical Research Letter 34, L06610. doi:10.1029/2006GL028851.
Lavaniegos, B.E., Ohman, M.D., 2003. Long-term changes in pelagic tunicates of the California current. Deep Sea Research 50, 2473–2498.
Lynn, R., 1967. Seasonal variation of temperature and salinity at 10 meters in the California current. California Cooperative Oceanic Fisheries Investigation Reports 11, 157–186.
Lynn, R., Simpson, J.J., 1987. The California current system: the seasonal variability of its physical characteristics. Journal of Geophysical Research 92, 12947–12966.
Lynn, R., Bograd, S., Chereskin, T., Huyer, A., 2003. Seasonal renewal of the California current: the spring transition off California. Journal of Geophysical Research 108 (C8), 3279. doi:10.1029/2003JC001787.
McClatchie, S., Goericke, R., Koslow, J.A., Schwing, F.B., Bograd, S.J., Charter, R., Watson, W., Lo, N., Hill, K., Gottschalk, J., L'Heureux, M., Xue, Y., Peterson, W.T., Emmett, R., Collins, C., Gaxiola-Castro, G., Durazo, R., Kahru, M., Mitchell, B.G., Hyrenbach, K.D., Sydeman, W.J., Bradley, R.W., Warzybok, P., Bjorkstedt, E., 2008. The state of the California current, 2007–2008: La Niña conditions and their effects on the ecosystem. California Cooperative Oceanic Fisheries Investigation Reports 49, 39–76.
Pérez-Brunius, P., López, A., Pineda, J., 2006. Hydrographic conditions near the coast of northwestern Baja California: 1997–2004. Continental Shelf Research 26, 885–901.
Pérez-Brunius, P., López, M., Parés-Sierra, A., Pineda, J., 2007. Comparison of upwelling indices off Baja California derived from three different wind data sources. California Cooperative Oceanic Fisheries Investigation Reports 48, 204–214.
Rykaczewski, R.R., Checkley, D.M., 2008. Influence of ocean winds on the pelagic ecosystem in upwelling regions. PNAS, doi:10.1073pnas.0711777105.
Soto-Mardones, L., Pares-Sierra, A., Garcia, J., Durazo, R., Hormazabal, S., 2004. Analysis of the mesoscale structure in the IMECOCAL region (off Baja California) from hydrographic, ADCP and altimetry data. Deep Sea Research Part II 51, 785–798.
Walstad, L.J., Allen, J.S., Kosro, P.M., Huyer, A., 1991. Dynamics of coastal transition zone through data assimilation studies. Journal of Geophysical Research 96, 14959–14977.
Wolter, K., Timlin, M.S., 1993. Monitoring ENSO in COADS with a seasonally adjusted principal component index. In: Proceedings of the of the 17th Climate Diagnostics Workshop, Norman, OK, NOAA/NMC/CAC, NSSL, Oklahoma Clim. Survey, CIMMS and the School of Meteor., University of Oklahoma. pp. 52–57.
Wolter, K., Timlin, M.S., 1998. Measuring the strength of ENSO events—how does 1997/98 rank? Weather 53 315–324.